Article

Not peer-reviewed version

Mechanistic Modeling Reveals Adaptive Photosynthetic Strategies of *Eichhornia crassipes*: Implications for Aquatic Plant Physiology and Invasion Dynamics

Lihua Liu , Xiaolong Yang , Piotr Robakowski , Zipiao Ye * , Shuangxi Zhou *

Posted Date: 22 April 2025

doi: 10.20944/preprints202504.1853.v1

Keywords: aquatic macrophytes; Eichhornia crassipes; photosynthetic plasticity; light stress adaptation; photoprotection; chlorophyll fluorescence; mechanistic modeling

 doi:10.20944/preprints202504.1853.v1

Article

Mechanistic Modeling Reveals Adaptive Photosynthetic Strategies of *Eichhornia crassipes*: Implications for Aquatic Plant Physiology and Invasion Dynamics

Lihua Liu [1,†], Xiaolong Yang [2,3,†], Piotr Robakowski [4], Zipiao Ye [5,6,*] and Shuangxi Zhou [7,*]

Running title: Photosynthetic Plasticity in Water Hyacinth

[1] College of Safety Engineering and Emergency Management, Nantong Institute of Technology, Nantong 226002, P. R. of China
[2] School of Life Sciences, Nantong University, Nantong 226019, P. R. of China
[3] State Key Laboratory of Environmental Chemistry and Ecotoxicology, Research Center for Eco-Environmental Sciences, Chinese Academy of Sciences, Beijing 100085, P. R. of China
[4] Department of Forestry, Poznan University of Life Sciences, Wojska Polskiego 71E St., 60–625 Poznan, Poland
[5] New Quality Productivity Research Center, Guangdong ATV College of Performing Arts, Deqing 526631, P. R. of China
[6] Math & Physics College, Jinggangshan University, Ji'an 343009, P. R. of China
[7] Department of Biological Sciences, Macquarie University, Sydney, NSW, Australia
* Correspondence: yezp@jgsu.edu.cn (Z.Y.); shuangxi.zhou@dpird.wa.gov.au (S.Z.)
† These authors equally contribute to this work.

Abstract: The invasive aquatic macrophyte *Eichhornia crassipes* (water hyacinth) exhibits exceptional adaptability across a wide range of light environments, yet the mechanistic basis of its photosynthetic plasticity under both high and low light stress remains poorly resolved. This study integrates chlorophyll fluorescence and gas exchange analyses to evaluate three photosynthetic models—rectangular hyperbola (RH), non-rectangular hyperbola (NRH), and the Ye mechanistic model—in capturing light-response dynamics in *E. crassipes*. The Ye model provided superior accuracy ($R^2 > 0.996$) in simulating net photosynthetic rate (P_n) and electron transport rate (J), outperforming empirical models that overestimated P_{nmax} by 36–46% and J_{max} by 1.5–24.7% and failed to predict saturation light intensity. Mechanistic analysis revealed that *E. crassipes* maintains high photosynthetic efficiency in low light (LUE_{max} = 0.030 mol mol^{-1} at 200 μmol photons m^{-2} s^{-1}) and robust photoprotection under strong light (NPQ_{max} = 1.375, PSII efficiency decline), supported by a large photosynthetic pigment pool (9.46 × 10^{16} molecules m^{-2}) and high eigen-absorption cross-section (1.91 × 10^{-21} m^2). Distinct thresholds for carboxylation efficiency (CE_{max} = 0.085 mol m^{-2} s^{-1}) and water-use efficiency ($WUE_{i\text{-}max}$ = 45.91 μmol mol^{-1} and WUE_{inst} = 1.96 μmol mmol^{-1}) highlighted its flexible energy management strategies. These results establish the Ye model as a reliable tool for characterizing aquatic photosynthesis and reveal how *E. crassipes* balances light harvesting and dissipation to thrive in fluctuating environments. Insights gained have implications for both understanding invasiveness and managing eutrophic aquatic systems.

Keywords: aquatic macrophytes; *Eichhornia crassipes*; photosynthetic plasticity; light stress adaptation; photoprotection; chlorophyll fluorescence; mechanistic modeling

1. Introduction

Aquatic macrophytes play pivotal roles in ecosystem functioning by mediating biogeochemical cycles and creating habitat heterogeneity within aquatic environments [1]. However, their

 doi:10.20944/preprints202504.1853.v1

photosynthetic traits fundamentally differ from terrestrial plants due to the unique environmental constraints, including rapid light attenuation in water [2], thermal fluctuations [3], and variable nutrient bioavailability [4]. Floating macrophytes such as *Eichhornia crassipes* (Mart.) Solms (water hyacinth) face a distinct challenge wherein their leaves, positioned at the air-water interface, are exposed to high light at the surface while simultaneously contending with self-shading and turbidity-driven light limitation [2]. This dual pressure necessitates adaptive strategies to balance photoprotection against intense sunlight with efficient light harvesting under low-light conditions—a dynamic critical to their ecological success.

E. crassipes, a free-floating perennial monocot native to South America, exemplifies a striking ecological paradox. Introduced to China as an ornamental species in the early 20th century, it has since become a pervasive invasive plant in ponds, reservoirs, and rivers [1]. Despite its notorious capacity for rapid proliferation, which often disrupts aquatic ecosystems, *E. crassipes* exhibits extraordinary physiological plasticity, enabling tolerance to a wide range of environmental stressors [5,6]. Central to this adaptability is its sophisticated photosynthetic apparatus, which integrates morphological traits (e.g., large floating leaves, vertical petioles) and biochemical adjustments to optimize light capture and carbon assimilation [6,7].

Plant leaves absorb, excite, transmit, and convert light energy based on the intrinsic properties of their light-harvesting pigments, including spatial structure and charge distribution [8]. The ecological dominance of *E. crassipes* appears closely associated with its ability to regulate photosynthesis [6], including strategies to tolerate or avoid light stress through increased leaf area, optimized photosynthetic efficiency via chloroplast arrangement and stomatal regulation, and vertical growth for enhanced light capture [6,9,10]. Under high light, its glossy leaves minimize photodamage through reflective surfaces and thermal dissipation mechanisms, while in shaded or turbid conditions, increased pigment density and chloroplast reconfiguration enhance light absorption efficiency [6,8]. These adaptations are governed by photochemical processes in photosystem II (PSII), where spatial organization of pigments and charge separation dynamics in reaction centers determine the quantum efficiency of electron transport [11,12]. Chlorophyll fluorescence analysis, a non-invasive method for probing PSII dynamics [13], has proven instrumental in characterizing these mechanisms in terrestrial plants. Recent advances integrating gas exchange, chlorophyll fluorescence, and photosynthetic modeling have clarified photoadaptive strategies in terrestrial systems by precisely characterizing photosynthetic capacity, electron transport dynamics, and PSII down-regulation [14–18]. However, analogous studies on aquatic macrophytes like *E. crassipes* are lacking, hindering our understanding of their unique photoadaptive physiology.

While terrestrial plants prioritize sustained light utilization, aquatic species like *E. crassipes* must balance efficient low-light harvesting with robust photoprotection. Previous studies highlight its capacity to maintain high photosynthetic efficiency across light gradients [6,9,19], yet the photophysical mechanisms enabling this plasticity remain unresolved. This study presents a comprehensive analysis of photosynthetic performance in *E. crassipes* using simultaneous measurements of chlorophyll fluorescence and gas exchange parameters using LI-6400 portable photosynthesis system. The purpose is to: a) quantify key photosynthetic light response characteristics; b) evaluate the applicability of three established photosynthetic models (rectangular hyperbola, non-rectangular hyperbola, and mechanistic models) for aquatic plants; c) investigate physiological foundation for its invasive success. Our findings provide novel insights into the photobiological adaptations of aquatic macrophytes and establish methodological frameworks for analyzing aquatic photosynthesis.

2. Materials and Methods

2.1. Plant Material

Mature *E. crassipes* plants were used for the experiment. They grew naturally a eutrophic pond adjacent to Jinggangshan University, Ji'an City, Jiangxi Province, China (27.09°N, 115.03°E; elevation 381.6 m). The plants were in a phase of vigorous vegetative growth, reaching heights of 31-52 cm and displaying 5-8 leaves with well-developed root system.

2.2. Gas Exchange and Chlorophyll Fluorescence Measurements

Measurements were taken on clear days in July 2019, from 8:30-11:30 and 14:00-17:30, at an average daytime temperature of 36°C. In this region, photosynthetically active radiation (PAR) typically

 doi:10.20944/preprints202504.1853.v1

reached around 2200 μmol photons m^{-2} s^{-1} in summer. Five to seven biologically independent plants with uniform growth were randomly selected, with fully expanded leaves from the upper canopy designated for measurement.

Prior to measurements, selected leaves were light-adapted for one hour under natural light. Simultaneous recordings of chlorophyll fluorescence and gas exchange parameters were obtained using a LI-6400 portable photosynthesis system equipped with a 6400-40 leaf chamber fluorometer (Li-Cor INC., USA). The open-path system maintained controlled conditions, including a CO_2 concentration of 380 μmol mol^{-1}, relative humidity of 50–70%, and air temperature within ± 1°C. A 16-step light intensity (I) gradient (2400, 2200, 2000, 1800, 1600, 1400, 1200, 1000, 800, 600, 400, 200, 150, 100, 50, and 0 μmol photons m^{-2} s^{-1}) was applied using the embedded "Flr Light Curve" automated protocol. Each light step included a 120-180 s equilibration period, followed by automated reference/sample cell matching. Steady-state measurements of net photosynthetic rate (P_n), electron transport rate (J), stomatal conductance (g_s), transpiration rate (T_r), intercellular CO_2 concentration (C_i), and PSII quantum efficiency (Φ_{PSII}), and non-photochemical quenching (NPQ) were recorded.

2.3. Photosynthesis Models and Calculations

2.3.1. Rectangular Hyperbola (RH) Model

The rectangular hyperbola model [20] is one of the classic models used to describe the photosynthetic light-response curve of plants. This model is characterized by its simplicity, minimal parameter requirements, and ease of computation. The mathematical representation of the RH model is given by:

$$P_n = \frac{\alpha I P_{nmax}}{\alpha I + P_{nmax}} - R_d \quad (1)$$

where P_{nmax} represents the maximum net photosynthetic rate, α is the initial slope of P_n-I response curve, and R_d is the dark respiration rate. Additionally, this model has been employed to characterize the response of J to I.

2.3.2. Non-Rectangular Hyperbola (NRH) Model

The NRH model [21,22], by introducing a curvature parameter (θ) to correct the "convexity" between low and high light intensities, thereby improving the accuracy of light-response curve fitting. When combined with the Farquhar–von Caemmerer–Berry (FvCB) biochemical model [23], the NRH model has become one of the core frameworks for modeling plant photosynthesis. The relationship between P_n and I in the NRH model is expressed as:

$$P_n = \frac{\alpha I + P_{nmax} - \sqrt{(\alpha I + P_{nmax})^2 - 4\alpha\theta I P_{nmax}}}{2\theta} - R_d \quad (2)$$

where θ represents the convexity of curve, and other parameters are as previously defined. Similar to the RH model, this model has also been applied to describe the response of J to I.

2.3.3. Photosynthetic Mechanistic Model (Ye Model)

The Ye model [24,25] is a mechanistic representation of the photosynthetic process, explicitly incorporating primary photophysical and photochemical reactions, including light absorption, exciton resonance transfer, quantum energy level transitions, and de-excitation. The model integrates photochemical reactions, exciton transfer, and physiological heat dissipation mechanisms. Through statistical weighting parameters, it quantitatively describes the partitioning of absorbed energy among photochemical reactions, thermal dissipation, and fluorescence. Importantly, this model can directly account for photoinhibition effects and provides an accurate representation of photosynthesis across the entire range of light intensities, from low light to saturation and inhibition [26–28]. The mathematical formulation of the Ye model is given by:

$$P_n = \frac{\alpha'\beta' N_0 \sigma_{ik} \varphi \eta}{s} \times \frac{1 - \frac{\left(1 - \frac{g_i}{g_k}\right)\sigma_{ik}\tau}{\xi_3 + (\xi_1 k_P + \xi_2 k_D)\tau} I}{1 + \frac{\left(1 + \frac{g_i}{g_k}\right)\sigma_{ik}\tau}{\xi_3 + (\xi_1 k_P + \xi_2 k_D)\tau} I} I - R_d \quad (3)$$

where α' represents the light energy distribution coefficient between PSII and PSI (dimensionless), β' is the leaf light absorption coefficient (dimensionless), N_0 is the number of light-harvesting pigment molecules, σ_{ik} is the intrinsic light absorption cross-section of light-harvesting pigment molecules (m^2), φ denotes the exciton utilization efficiency (dimensionless), η is the efficiency of photosynthetic electron transport (its reciprocal represents the number of electron required to assimilate one CO_2

 doi:10.20944/preprints202504.1853.v1

molecule), S represents the measured leaf area (m^2). g_i and g_k are the energy level degeneracies of the light-harvesting pigment molecule in ground and excited states, respectively (dimensionless). ξ_1, ξ_2 and ξ_3 are the statistical weighting factors for exciton transfer to photochemistry, heat dissipation, and fluorescence, respectively (dimensionless). k_P is the photoreaction rate constant (s^{-1}). k_D is the heat dissipation rate constant (s^{-1}). τ represents the average lifetime of the light-harvesting pigment molecule in the lowest excited state (s^{-1}) [24,25].

According to Equation (3), P_n depends on multiple biophysical parameters, including α', β', N_0, σ_{ik}, φ, η, S, g_i, g_k, ξ_1, ξ_2, ξ_3, k_P, k_D, and τ. Under steady-state conditions, these parameters are intrinsic to the plant species but may vary under different environmental conditions. To facilitate practical applications, three aggregate parameters are introduced to simplify Equation (3): $\alpha_p = \frac{\alpha'\beta' N_0 \sigma_{ik} \varphi \eta}{S}$ (μmol electrons (μmol photons)$^{-1}$), $\beta_p = \frac{\left(1-\frac{g_i}{g_k}\right)\sigma_{ik}\tau}{\xi_3+(\xi_1 k_P+\xi_2 k_D)\tau}$ (m^2 s (μmol photons)$^{-1}$), and $\gamma_p = \frac{\left(1+\frac{g_i}{g_k}\right)\sigma_{ik}\tau}{\xi_3+(\xi_1 k_P+\xi_2 k_D)\tau}$ (m^2 s (μmol photons)$^{-1}$).

$$P_n = \alpha_p \frac{1-\beta_p I}{1+\gamma_p I} I - R_d \quad (4)$$

where α_p is the initial slope of the P_n-I response curve, while β_p and γ_p are parameters characterizing light limitation and light saturation, respectively.

The photosynthetic quantum efficiency (P'_n), defined as the number of CO_2 molecules fixed per photon absorbed at a given I, is derived from Equation (4) as:

$$P'_n = \frac{\gamma_p - \alpha_p I^2}{(\gamma_p+\beta_p I+\alpha_p I^2)^2} \quad (5)$$

The maximum P_n (P_{nmax}) is determined by:

$$P_{nmax} = \alpha_p \left(\frac{\sqrt{\beta_p+\gamma_p}-\sqrt{\beta_p}}{\gamma_p} \right)^2 - R_d \quad (6)$$

while the saturation I (I_{sat}) is given by:

$$I_{sat} = \frac{\sqrt{(\beta_p+\gamma_p)/\beta_p - 1}}{\gamma_p} \quad (7)$$

Ye et al. (2013) also established the relationship between J and I in their photosynthetic mechanistic model using the following equation:

$$J = \alpha_e \frac{1-\beta_e I}{1+\gamma_e I} I \quad (8)$$

where α_e is the initial slope of the J-I response curve, β_e is PSII dynamics down-regulation coefficient, and γ_e are the saturation coefficient.

The maximum J (J_{max}) is determined by:

$$J_{max} = \alpha_e \left(\frac{\sqrt{\beta_e+\gamma_e}-\sqrt{\beta_e}}{\gamma_e} \right)^2 \quad (9)$$

while the saturation I ($I_{e\text{-}sat}$) is given by:

$$I_{e\text{-}sat} = \frac{\sqrt{(\beta_e+\gamma_e)/\beta_e - 1}}{\gamma_e} \quad (10)$$

Additionally, by incorporating chlorophyll content (unit: mg m^{-2}), Equation (8) can be used to simulate J-I curves, allowing the extraction of key traits characterizing light-harvesting pigment molecules, including the total photosynthetic pigment molecules (N_0), the eigen-absorption cross-section of photosynthetic pigment molecules (σ_{ik}), the minimum average lifetime of the lowest excited-state photosynthetic pigment molecules (τ_{min}), the effective absorption cross-section of pigment molecules (σ'_{ik}), and the total excited-state pigment molecules (N_k) [25]. Moreover, building upon the P_n-I and J-I mechanistic models, Ye and Yang et al. developed quantitative models describing the light response of light-use efficiency (LUE) [29], carboxylation efficiency (CE), intrinsic and instantaneous WUE (WUE_i and WUE_{inst}, respectively) [30], Φ_{PSII} and NPQ [18]. These interconnected models provide a comprehensive framework for quantifying plant photosynthetic physiology, as detailed previously.

2.4. Statistical Analysis

Non-linear regression was performed to fit P_n-I, J-I, NPQ-I, Φ_{PSII}-I, LUE-I, CE-I, WUE_i-I, and WUE_{inst}-I curves using the *Photosynthesis Model Simulation Software* (PMSS, Jinggangshan University) (http://photosynthetic.sinaapp.com/index.html-Chinese/English version). Goodness of fit of the three

 doi:10.20944/preprints202504.1853.v1

models was evaluated by the coefficient of determination (R^2 = 1 - SSE/SST, where SST is the total sum of squares and SSE is the error sum of squares), Akaike's information criterion (*AIC*), and Mean absolute Error (MAE = $\frac{1}{n}\sum_{i=1}^{n}|\hat{y}_i - y_i|$, where $\hat{y}_i$ is the fitted values from model and y_i is the measured values). A one-way analysis of variance (ANOVA) was conducted using SPSS Statistics 24.0 to compare differences between the model-fitted and measured values, with statistical significance set at $p < 0.05$. The ratio of J_{max} to P_{nmax} can be used to estimate the apparent number of electrons required to assimilate one molecule of CO_2 (n_a), providing an indicator of the photosynthetic electron utilization efficiency in plant leaves. Data are presented as mean ± *SE* (n = 4).

3. Results

3.1. Photosynthetic and Electron Transport Responses

The photosynthetic light-response dynamics of *E. crassipes* were rigorously assessed through coupled chlorophyll fluorescence and gas exchange analyses. **Figure 1A–C** illustrates the light-dependent progression of net photosynthetic rate (P_n), which exhibited a hyperbolic increase with increasing I, saturating at approximately 2000 μmol photons m^{-2} s^{-1} without photoinhibition. The Ye mechanistic model demonstrated superior goodness-of-fit (R^2 = 0.9963, MAE = 0.40, *AIC* = 4.34) in replicating the P_n-I curve (**Figure 1C**), with no statistically significant deviation between modeled and observed P_{nmax} (24.64 ± 1.08 vs. 24.70 ± 1.01 μmol CO_2 m^{-2} s^{-1}, $p > 0.05$, Table 1). In contrast, both rectangular (RH) and non-rectangular hyperbola (NRH) models overestimated P_{nmax} by 45.7% and 36.4%, respectively ($p < 0.05$), and failed to yield saturation light intensity (I_{sat}), highlighting their limitations in capturing high-light dynamics (**Figure 1A-B, Table 1**).

Parallel analysis of electron transport rate (J) revealed a biphasic response to I, peaking at 186.07 ± 10.04 μmol CO_2 m^{-2} s^{-1}, and then gradually declined, indicating dynamic downregulation of PSII activity (**Figure 1D–F**). The Ye model precisely simulated this trajectory (R^2 = 0.9979, MAE = 2.12, *AIC* = 19.29), whereas RH and NRH models diverged markedly at supra-optimal light intensity, overestimating J_{max} by 24.7% and 1.5%, respectively (**Table 1**). This also leaded to a significant overestimation of the value of apparent electron requirement for CO_2 assimilation (n_a) in both models. However, the n_a value from the Ye model closely aligned with the measured (**Table 1**).

 doi:10.20944/preprints202504.1853.v1

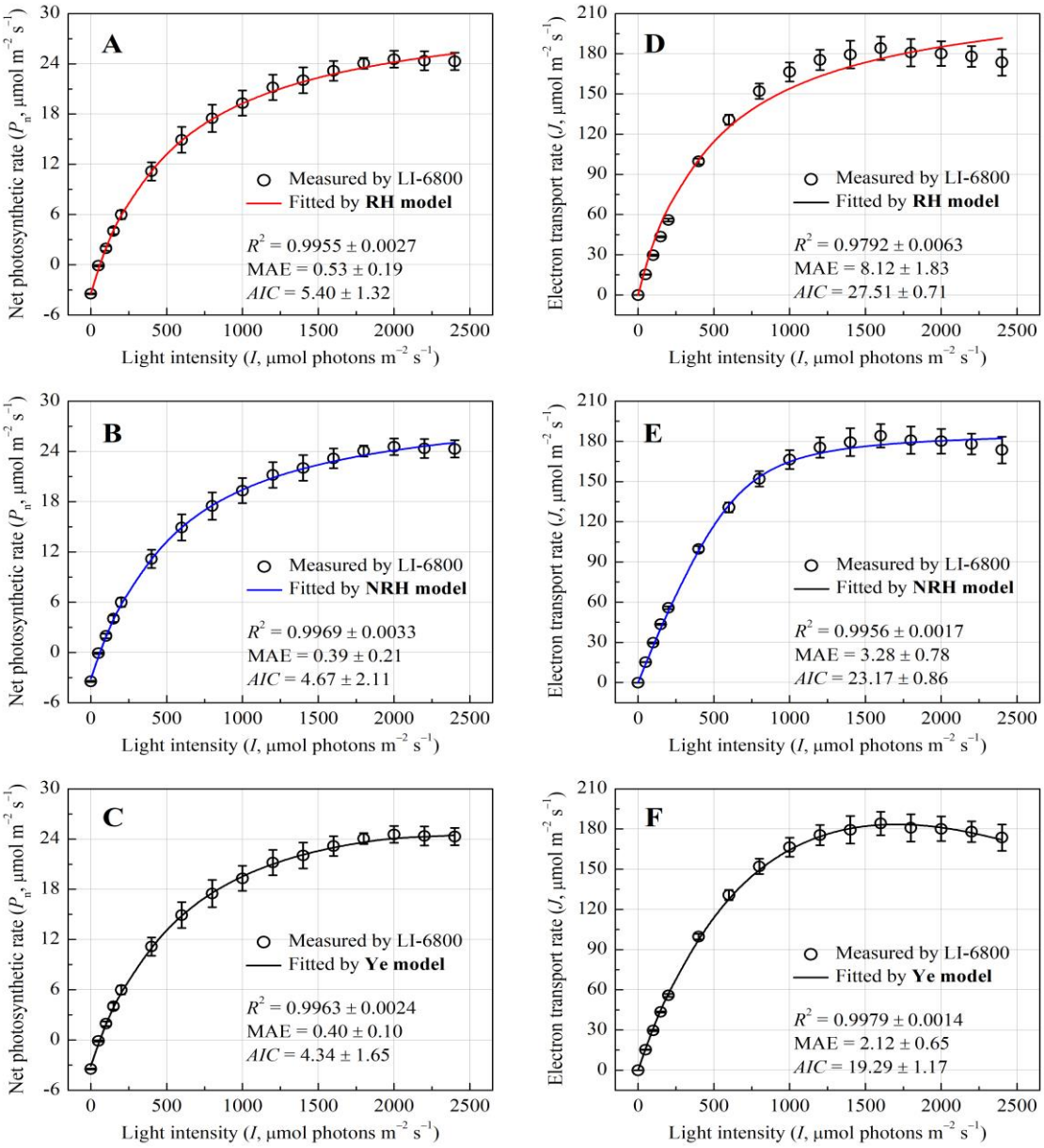

Figure 1. Light-response curves of the net photosynthetic rate (P_n) and electron transport rate (J) for *E. crassipes*. The curves were simulated by RH model, NRH model, and Ye Model, respectively.

Table 1. Fitted and measured values of traits defining P_n–I and J–I curves of E. crassipes. Values are means ± SE (n = 4). Within each row, values with different letters are significantly different ($p < 0.05$).

Traits	Fitted value			Measured value
	RH Model	NRH Model	Ye Model	
α_p (μmol mol^{-1})	0.0659 ± 0.0111a	0.0522 ± 0.0058a	0.0528 ± 0.0107a	—
P_{nmax} (μmol m^{-2} s^{-1})	35.93 ± 1.33a	33.70 ± 1.65a	24.64 ± 1.08b	24.70 ± 1.01b
I_{sat} (μmol m^{-2} s^{-1})	—	—	2520.41 ± 243.03a	2200.00 ± 81.65a
I_c (μmol m^{-2} s^{-1})	58.78 ± 3.59a	60.02 ± 3.33a	54.17 ± 2.45a	53.06 ± 2.11a
R_d (μmol m^{-2} s^{-1})	3.41 ± 0.46a	2.91 ± 0.24b	3.46 ± 0.16a	3.46 ± 0.06a
α_e (μmol mol^{-1})	0.4658 ± 0.0109a	0.2779 ± 0.0052c	0.3424 ± 0.0076b	—
J_{max} (μmol m^{-2} s^{-1})	232.08 ± 16.78a	188.85 ± 11.66b	184.10 ± 10.84b	186.07 ± 10.04b
$I_{e\text{-}sat}$ (μmol m^{-2} s^{-1})	—	—	1699.64 ± 40.39a	1750.00 ± 170.78a
n_a	6.45 ± 0.34b	5.62 ± 0.31b	7.46 ± 0.12a	7.52 ± 0.12a
σ_{ik} (10^{-21} m^2)	—	—	1.91 ± 0.04	—
τ_{min} (ms)	—	—	11.53 ± 1.27	—
N_0 (10^{16} m^2)	—	—	9.46 ± 0.08	—

 doi:10.20944/preprints202504.1853.v1

Chl content (mg m^{-2})	—	—	—	707.34 ± 5.86

3.2. Quantum Yield and Photophysical Traits of Light-Harvesting Pigment Molecules

Photosynthetic quantum efficiency (P'_n), reflecting the efficiency of light energy conversion, decreased from 0.023 ± 0.002 to –0.47×10^{-3} μmol CO_2 μmol photons^{-1} with increasing I, indicating diminished light utilization (**Figure 2A**). The negative P'_n at I = 2400 μmol photons m^{-2} s^{-1} indicates that respiratory CO_2 release exceeded photosynthetic CO_2 fixation, which was supported by the stabilization of respiratory rate in the light (R_{Light}) at 2.97% of P_n under saturating light (**Figure 2B**). Mechanistic modeling of *J-I* curves resolved intrinsic photophysical parameters of light-harvesting pigments. As shown in **Table 1**, the total photosynthetic pigment pool (N_0 = 9.46 ± 0.08 × 10^{16}) and eigen-absorption cross-section (σ_{ik} = 1.91 ± 0.04 × 10^{-21} m^2) underscored robust light-capturing capacity. The minimum average lifetime of the lowest excited-state pigment molecules (τ_{min}) was 11.53 ± 1.27 ms. The total excited-state pigment molecules (N_k) increased with I (**Figure 2C**), suggesting a gradual shift toward energy dissipation rather than abrupt saturation. Despite a 73.8% reduction in effective absorption cross-section (σ'_{ik}) under high light (0.5 × 10^{-21} m^2 at I = 2000 μmol photons m^{-2} s^{-1}, **Figure 2D**), residual absorption capacity remained sufficient to sustain photosynthetic activity, reflecting adaptive plasticity in light harvesting.

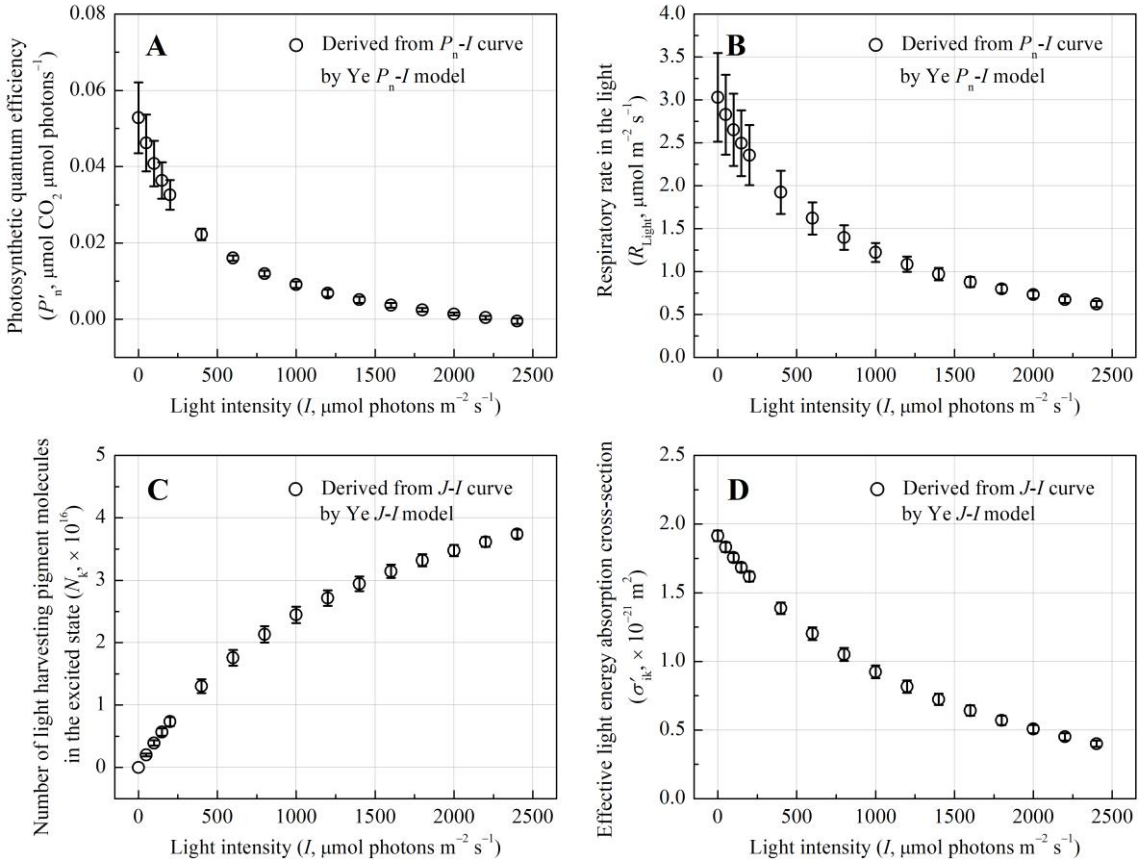

Figure 2. Light-response curves of the photosynthetic quantum efficiency (P'_n), respiratory rate in the light (R_{Light}), total excited-state pigment molecules (N_k) and effective absorption cross-section (σ'_{ik}) for *E. crassipes*.

3.3. Photoprotection and Metabolic Efficiency Dynamics

Non-photochemical quenching (*NPQ*) increased monotonically to 1.375 ± 0.062 at I = 2350 μmol photons m^{-2} s^{-1} (**Figure 3A**), consistent with enhanced thermal dissipation under high light. This photoprotective response coincided with a decline in PSII quantum efficiency (Φ_{PSII}) from 0.762 ± 0.007 to 0.412 ± 0.011 (**Figure 3B**), suggesting reduced photochemical efficiency as light saturation intensified. Light-use efficiency (*LUE*) followed a typical peaked response, with a sharp rise at low light and a gradual decline beyond saturation at approximately 200 μmol photons m^{-2} s^{-1} (**Figure 3C**), while carboxylation efficiency (*CE*) reached its maximum 0.085 mol m^{-2} s^{-1} at I = 2200 μmol photons m^{-2} s^{-1} (**Figure 3D**), reflecting distinct thresholds for light capture and CO_2 assimilation. Water-use metrics

 doi:10.20944/preprints202504.1853.v1

exhibited analogous saturation patterns, with intrinsic water-use efficiency (WUE_i) plateauing at I = 1600 μmol photons m^{-2} s^{-1} (45.91 ± 6.28 μmol mol^{-1}, **Figure 3E**) and instantaneous WUE (WUE_{inst}) stabilizing earlier at I = 1400 μmol photons m^{-2} s^{-1} (1.96 ± 0.29 $mmol^{-1}$, **Figure 3F**).

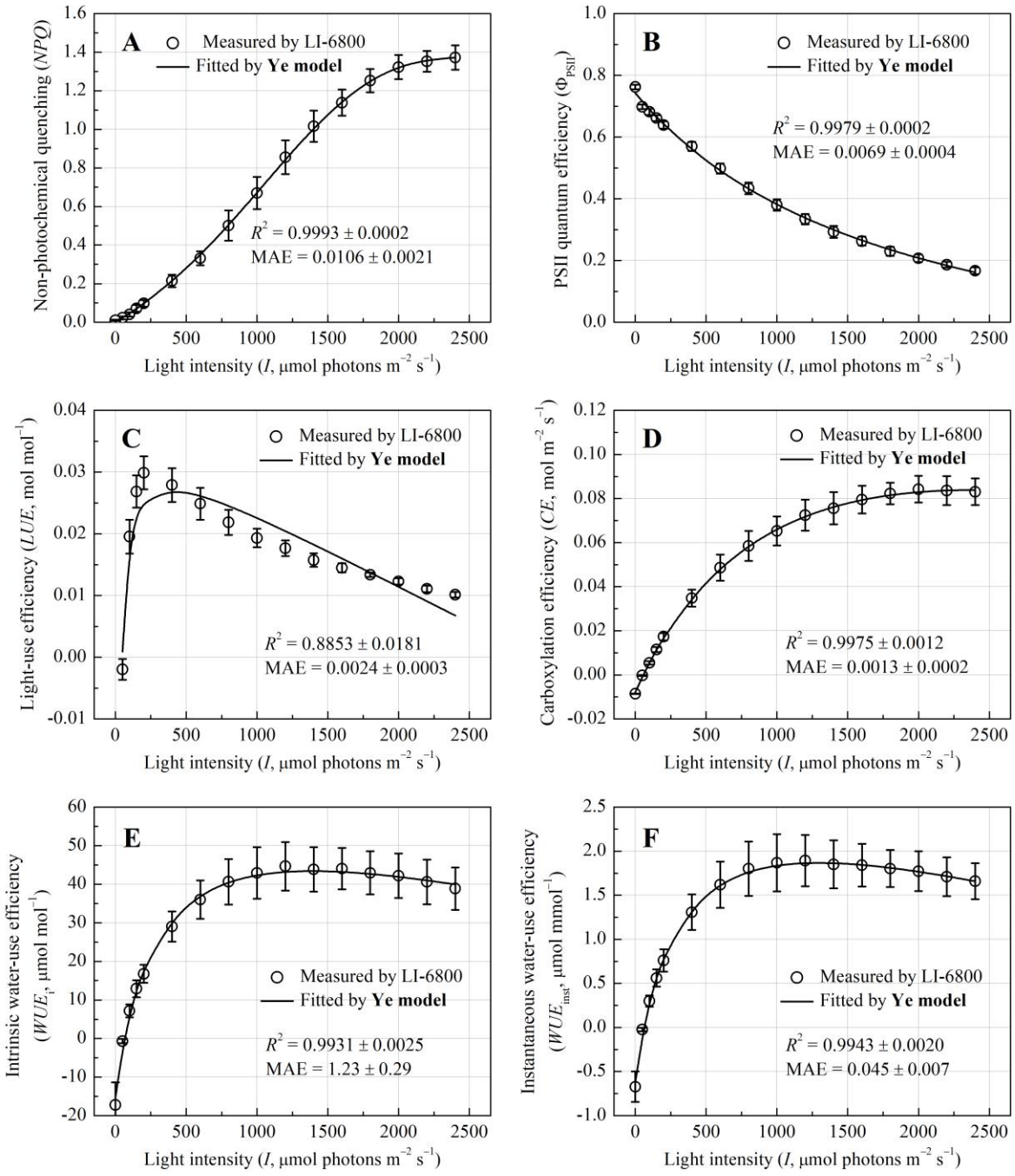

Figure 3. Light-response curves of the non-photochemical quenching (NPQ), PSII quantum efficiency (Φ_{PSII}), light-use efficiency (LUE), carboxylation efficiency (CE), and intrinsic and instantaneous water-use efficiency (WUE_i and WUE_{inst}, respectively) for *E. crassipes*.

Critically, derivative models from the Ye mechanism framework (e.g., NPQ-I, Φ_{PSII}-I, CE-I, WUE_i-I, WUE_{inst}-I) accurately simulated photoprotective and metabolic responses ($R^2 > 0.99$) (**Figure 3**). Fitted NPQ_{max}, CE_{max}, $WUE_{i\text{-}max}$, and $WUE_{inst\text{-}max}$, and their saturation light intensities, closely matched measured values ($p > 0.05$) (**Table 2**). While the Φ_{PSII}-I model slightly underestimated $\Phi_{PSII\text{-}max}$, the LUE-I model only moderately captured LUE changes, exhibiting larger discrepancies compared to other parameters.

Table 2. Fitted and measured values of photoprotection and physiological traits of *E. crassipes*. *Values are means ± SE (n = 4). Within each row, values with different letters are significantly different (p < 0.05).*

 doi:10.20944/preprints202504.1853.v1

Traits	Fitted value	Measured value
NPQ_{max}	1.366 ± 0.058a	1.375 ± 0.062a
$I_{NPQ\text{-}sat}$ (μmol m^{-2} s^{-1})	2278.76 ± 41.25a	2350.00 ± 50.00a
$\Phi_{PSIImax}$	0.743 ± 0.007b	0.762 ± 0.007a
LUE_{max} (mol mol^{-1})	0.027 ± 0.002a	0.030 ± 0.003a
$I_{LUE\text{-}sat}$ (μmol m^{-2} s^{-1})	384.65 ± 17.60a	250.00 ± 50.00b
CE_{max} (mol m^{-2} s^{-1})	0.084 ± 0.006a	0.085 ± 0.006a
$I_{CE\text{-}sat}$ (μmol m^{-2} s^{-1})	2242.99 ± 82.55a	2000.00 ± 81.65b
$WUE_{i\text{-}max}$ (μmol mol^{-1})	44.17 ± 6.09a	45.91 ± 6.28a
$I_{i\text{-}sat}$ (μmol m^{-2} s^{-1})	1621.82 ± 267.39a	1500.00 ± 173.21a
$WUE_{inst\text{-}max}$ (μmol mmol^{-1})	1.88 ± 0.28a	1.96 ± 0.29a
$I_{inst\text{-}sat}$ (μmol m^{-2} s^{-1})	1391.42 ± 139.03a	1300.00 ± 173.21a

4. Discussion

4.1. Applicability of Ye Mechanistic Model in Aquatic Plants Photosynthesis

Our results demonstrate the superior performance of Ye mechanistic model in the simulating photosynthetic light-response curves of *E. crassipes* compared to traditional empirical models (RH, NRH), aligning with previous studies that have validated the Ye model in various plant species, including terrestrial plants [26–28,30,31], cyanobacteria [32], and eukaryotic algae [33]. The Ye model's advantage lies in its detailed incorporation of both photophysical and photochemical processes. Specifically, it accounts for light absorption (σ_{ik}), exciton transfer efficiency (φ), and energy dissipation dynamics (k_D, τ), all critical for accurately representing aquatic photosynthesis in variable light conditions.

While the RH and NRH models provided reasonable approximations under low light, they fell short in capturing high-light saturation and the dynamic down-regulation of PSII. These models overestimated the P_{nmax} by 36–46% and the J_{max} by 1.5–24.7% because they assume linear or hyperbolic light responses without accounting for the underlying physiological mechanisms of photosynthesis [16]. These findings align with prior critiques of empirical models in terrestrial systems [16,34–36], which lack the flexibility to simulate dynamic photoinhibition or species-specific photoprotective strategies. In contrast, the Ye model's parameterization of N_k (total excited-state pigments), τ_{min} (the minimum average lifetime of excited-state pigments), and σ'_{ik} (effective absorption cross-section)—explains how *E. crassipes* rapidly dissipates excess energy as heat under high light, thereby avoiding photodamage. In addition, the close alignment between modeled and observed J_{max}/P_{nmax} ratio (n_a = 7.46 vs. 7.52) in *E. crassipes* underscores the Ye model's ability to quantify electron transport efficiency. This ratio reflects the balance between linear electron flow (driven by PSII activity) and carboxylation efficiency, a relationship inherently modulated by large N_0 and adaptive *NPQ* [37]. Traditional models, which oversimplify electron transport as a static function of light, fail to resolve these interdependencies. The Ye model's mechanistic basis thus provides a critical tool for studying aquatic plants, where environmental variability (e.g., light fluctuations, nutrient gradients) demands precise representation of energy allocation and stress responses.

4.2. Evolutionary Adaptations of E. crassipes

The photosynthetic performance of *E. crassipes* reveals evolutionary adaptations that differentiate it from native aquatic macrophytes. As shown in **Table 3**, its P_{nmax} and I_{sat} exceed values reported for other aquatic plants like *Nymphoides peltate*, *Nelumbo nucifera*, and *Phragmites australis* [38–40], which show P_{nmax} values < 20 μmol CO_2 m^{-2} s^{-1} and earlier photoinhibition thresholds. Even its photosynthetic capacity exceeds that of some common C_3 plants such as *Oryza sativa* [41], *Tamarix ramosissima* [42], *Solanum lycopersicum* L. [43], *Malus pumila* Mill. [44], and *Glycine max* L. (Merr.) [45]. The I_{sat} is close to C_4 maize [19] and exceeds C_4 sorghum [16]. These traits suggest that *E. crassipes* has evolved more efficient mechanisms for light absorption and energy dissipation, making it particularly competitive in nutrient-rich, high-light environments. The plant's large photosynthetic pigment pool (9.46 × 10^{16} molecules m^{-2}) and high eigen-absorption cross-section (1.91 × 10^{-21} m^2) enhance photon absorption efficiency, which is coupled with dynamic photoprotective responses, such as *NPQ*, to prevent photodamage under high light. Interestingly, regional variation in photosynthetic capacity, such as the higher P_{nmax} observed in *E. crassipes* populations in Nanjing, China (32.03°N, 118.88°E;

 doi:10.20944/preprints202504.1853.v1

elevation 10 m) [19] and in Federal University of Lavras, state of Minas Gerais, Brazil. (19.913°S, 43.941°W; elevation 830 m) [6], indicates the species' ability to adapt to local light conditions. This adaptability contrasts sharply with native species like *N. peltate* [38], which exhibit more rigid physiological responses to environmental gradients, further emphasizing the ecological flexibility of *E. crassipes*.

Table 3. *E. crassipes* compared to other plants in photosynthetic ability.

Plants	P_{nmax}	I_{sat}	J_{max}	$I_{e\text{-}sat}$	Reference
E. crassipes	23.1–30.8	—	—	—	[6]
E. crassipes	34.5 ± 0.72	2358 ± 69	—	—	[19]
E. crassipes	24.70 ± 1.01	2200.0 ± 81.7	186.1 ± 10.0	1750.0 ± 170.8	This study
Nymphoides peltate	12.66	219.98	—	—	[38]
Nelumbo nucifera	7.1–9.2	—	—	—	[39]
Phragmites australis	9.0~19.5	924.1–2186.3	—	—	[40]
Oryza sativa L.	17.51–27.89	≈ 2000	—	—	[41]
Oryza sativa L. (Kitaake)	19.56 ± 0.62	1641 ± 32.0	—	—	[19]
Tamarix ramosissima	17.2–24.4	957–1360	—	—	[42]
Solanum lycopersicum L.	6.34–17.82	—	—	—	[43]
Malus pumila Mill.	15.25–20.29	1413.8–1874.9	—	—	[44]
Glycine max L. (Merr.)	19.73	1800	143.51 ± 5.21	1601.6 ± 0.64	[45]
Zea mays L. (Nongda 108)	30.36 ± 0.42	2550 ± 37.0	—	—	[19]
Sorghum bicolor L. (KFJT-4)	37.49 ± 0.90	1866.7 ± 33.3	170.15 ± 4.451	640.0 ± 74.83	[16,18]
Sorghum bicolor L. (KFJT-1)	—	—	133.84 ± 5.521	600.0 ± 63.24	[18]

4.3. Synergistic Efficiency Metrics Supports Invasiveness of E. crassipes

The integration of key efficiency metrics—light-use efficiency (*LUE*), water-use efficiency (*WUE*), and carboxylation efficiency (*CE*)—provides a comprehensive physiological framework for understanding the invasiveness of *E. crassipes*. The species' high LUE_{max} (0.030 mol mol^{-1}) at low light intensity (approximately 200 μmol photons m^{-2} s^{-1}), coupled with a sharp decline in *LUE* at higher light levels, indicates its strategic shift toward photoprotection rather than carbon fixation as light intensity increases. This plasticity enables *E. crassipes* to thrive under variable light conditions while maintaining efficient resource utilization. Moreover, the species exhibits superior *WUE*, as reflected in both intrinsic *WUE* (WUE_i) and instantaneous *WUE* (WUE_{inst}). These metrics suggest that *E. crassipes* effectively regulates stomatal conductance to balance CO_2 uptake and water conservation, a critical strategy for survival in eutrophic environments. This efficient use of light and water, combined with the species' high J_{max}, places *E. crassipes* in direct competition with native macrophytes like *P. australis*, which exhibit lower *CE* and less effective photoprotective mechanisms [40]. However, under high light (>1600 μmol photons m^{-2} s^{-1}), as observed in most C_3 plants, *E. crassipes* also exhibited significant PSII dynamic down-regulation [18,46].

5. Conclusions

In conclusion, this study highlights the utility of the Ye mechanistic model in elucidating the complex photobiological adaptations that contribute to the ecological success of *E. crassipes*. By integrating chlorophyll fluorescence and gas exchange data, we provide a holistic view of the species' photosynthetic performance, linking molecular-level mechanisms to its ecosystem-level invasiveness. The findings underscore the critical role of efficient light-harvesting and energy dissipation in enabling *E. crassipes* to dominate eutrophic, high-light environments. Future research should extend this approach to other aquatic macrophytes, particularly invasive species, to identify universal physiological traits that predict ecological success and inform management strategies in aquatic ecosystems.

 doi:10.20944/preprints202504.1853.v1

Author Contributions: L.L. and X.Y. conducted the experiment and drafted the manuscript. X.Y. and Z.Y. performed the statistical analysis. X.Y., Z.Y., P. R. and S.Z. performed model calculations and statistical analysis. Funding for the research was secured by X.Y. and Z.Y. All authors critically reviewed and revised the manuscript with new data sets and contributed substantially to the completion of the present study. All authors read and approved the final manuscript.

Funding: This work was supported by the Natural Science Foundation of China (Grant No. 32260063 and 31960054).

References

1. Fan, D.; Schwinghamer, T.; Liu, S.; Xia, O.; Ge, C.; Chen, Q.; Smith, D. L. Characterization of endophytic bacteriome diversity and associated beneficial bacteria inhabiting a macrophyte *Eichhornia crassipes*. *Front. Plant Sci.* **2023,** *14*, 1176648.
2. López-Pozo, M.; Adams, W. W.; Polutchko, S. K.; Demmig-Adams, B. Terrestrial and floating aquatic plants differ in acclimation to light environment. *Plants* **2023,** *12*, 1928.
3. Pilon, J.; Santamaría, L. Clonal variation in the thermal response of the submerged aquatic macrophyte *Potamogeton pectinatus*. *J. Ecol.* **2002,** *90*, 141-152.
4. Pasos-Panqueva, J.; Baker, A.; Camargo-Valero, M. A. Unravelling the impact of light, temperature and nutrient dynamics on duckweed growth: A meta-analysis study. *J. Environ. Manage.* **2024,** *366*, 121721.
5. Meneguelli-Souza, A. C.; Vitória, A. P.; Vieira, T. O.; Degli-Esposti, M. S. O.; Souza, C. M. M. Ecophysiological responses of *Eichhornia crassipes* (Mart.) Solms to As^{5+} under different stress conditions. *Photosynthetica* **2016,** *54*, 243-250.
6. Pereira, F. J.; Castro, E. M.; Oliveira, C.; Pires, M. F.; Pereira, M. P.; Ramos, S. J.; Faquin, V. Lead tolerance of water hyacinth (*Eichhornia crassipes* Mart. - Pontederiaceae) as defined by anatomical and physiological traits. *An. Acad. Bras. Cienc.* **2014,** *86*, 1423-1433.
7. Downing-Kunz, M.; Stacey, M. Flow-induced forces on free-floating macrophytes. *Hydrobiologia* **2011,** *671*, 121-135.
8. Kühlbrandt, W.; Wang, D. N.; Fujiyoshi, Y. Atomic model of plant light-harvesting complex by electron crystallography. *Nature* **1994,** *367*, 614-621.
9. Ripley, B. S.; Muller, E.; Behenna, M.; Whittington-Jones, G. M.; Hill, M. P. Biomass and photosynthetic productivity of water hyacinth (*Eichhornia crassipes*) as affected by nutrient supply and mirid (*Eccritotarus catarinensis*) biocontrol. *Biol. Control* **2006,** *39*, 392-400.
10. Maranho, L. T.; Gomes, M. P. Morphophysiological adaptations of aquatic macrophytes in wetland-based sewage treatment systems: strategies for resilience and efficiency under environmental stress. *Plants* **2024,** *13*, 2870.
11. Long, S. P.; Taylor, S. H.; Burgess, S. J.; Carmo-Silva, E.; Lawson, T.; De Souza, A. P.; Leonelli, L.; Wang, Y. Into the shadows and back into sunlight: Photosynthesis in fluctuating light. *Ann. Rev. Plant Biol.* **2022,** *73*, 617-648.
12. Ruan, M.; Li, H.; Zhang, Y.; Zhao, R.; Zhang, J.; Wang, Y.; Gao, J.; Wang, Z.; Wang, Y.; Sun, D.; Ding, W.; Weng, Y. Cryo-EM structures of LHCII in photo-active and photo-protecting states reveal allosteric regulation of light harvesting and excess energy dissipation. *Nat. Plants* **2023,** *9*, 1547-1557.
13. Baker, N. R. Chlorophyll fluorescence: a probe of photosynthesis in vivo. *Annu. Rev. Plant Biol.* **2008,** *59*, 89-113.
14. Yin, X.; Sun, Z.; Struik, P. C.; Gu, J. Evaluating a new method to estimate the rate of leaf respiration in the light by analysis of combined gas exchange and chlorophyll fluorescence measurements. *J. Exp. Bot.* **2011,** *62*, 3489-3499.
15. Yin, X. Y.; Struik, P. C. Theoretical reconsiderations when estimating the mesophyll conductance to CO_2 diffusion in leaves of C_3 plants by analysis of combined gas exchange and chlorophyll fluorescence measurements. *Plant Cell Environ.* **2009,** *32*, 1513-1524.
16. Yang, X.-L.; Ma, X.-F.; Ye, Z.-P.; Yang, L.-S.; Shi, J.-B.; Wang, X.; Zhou, B.-B.; Wang, F.-B.; Deng, Z.-F. Simulating short-term light responses of photosynthesis and water use efficiency in sweet sorghum under varying temperature and CO_2 conditions. *Front. Plant Sci.* **2024,** *15*, 1291630.

 doi:10.20944/preprints202504.1853.v1

17. Ye, Z. P.; Kang, H. J.; An, T.; Duan, H. L.; Wang, F. B.; Yang, X. L.; Zhou, S. X. Modeling light response of electron transport rate and its allocation for ribulose biphosphate carboxylation and oxygenation. *Front. Plant Sci.* **2020,** *11*, 581851.
18. Yang, X.-L.; An, T.; Ye, Z.-W.-Y.; Kang, H.-J.; Robakowski, P.; Ye, Z.-P.; Wang, F.-B.; Zhou, S.-X. Modeling light response of effective quantum efficiency of photosystem II for C_3 and C_4 crops. *Front. Plant Sci.* **2025,** *16*, 1478346.
19. Xia, L.; Jianchu, Z.; Shaohua, Y.; Chenggang, R.; Man, W.; Wei, C.; Jing, S.; Puping, Z. Dynamics of photosynthesis in *Eichhornia crassipes* dolms of Jiangsu of China and their influencing factors. *African Journal of Biotechnology* **2010,** *9*, 7302-7311.
20. Baly, E. C. C. The kinetics of photosynthesis. *Proceedings of the Royal Society of London* **1935,** *149*, 596-596.
21. Farquhar, G. D.; Wong, S. C. An empirical model of stomatal conductance. *Aust. J. Plant Physiol.* **1984,** *11*, 191-210.
22. Thornley, J. H. M. *Mathematical Models in Plant Physiology: A quantitative approach to problems in plant and crop physiology (Experimental botany)* London, UK: Academic Press, 1976.
23. Farquhar, G. D.; von Caemmerer, S.; Berry, J. A. A biochemical model of photosynthetic CO_2 assimilation in leaves of C_3 species. *Planta* **1980,** *149*, 78-90.
24. Ye, Z. P.; Suggett, J. D.; Robakowski, P.; Kang, H. J. A mechanistic model for the photosynthesis-light response based on the photosynthetic electron transport of photosystem II in C_3 and C_4 species. *New Phytol.* **2013,** *199*, 110-120.
25. Ye, Z. P. Nonlinear optical absorption of photosynthetic pigment molecules in leaves. *Photosynth. Res.* **2012,** *112*, 31-37.
26. Martínez-García, E.; Rubio, E.; García-Morote, F. A.; Andrés-Abellán, M.; Miettinen, H.; López-Serrano, F. R. Net ecosystem production in a Spanish black pine forest after a low burn-severity fire: Significance of different modelling approaches for estimating gross primary production. *Agr. Forest Meteorol.* **2017,** *246*, 178-193.
27. Atsushi, S.; Tatsuya, K.; Shigeto, T.; Masashi, Y. Effect of temperature on photosynthesis characteristics in the passion fruits 'Summer Queen' and 'Ruby Star'. *Horticult. J.* **2017,** *86*, 194-199.
28. Liu, S.; Liu, W.; Shi, X.; Li, S.; Hu, T.; Song, L.; Wu, C. Dry-hot stress significantly reduced the nitrogenase activity of epiphytic cyanolichen. *Sci. Total Environ.* **2018,** *619-620*, 630-637.
29. Ye, Z. P.; Zhang, H. L.; Huang, Z. A.; Yang, X. L.; Kang, H. J. Model construction of light use efficiency and water use efficiency based on a photosynthetic mechanistic model of light response. *J. Plant Physiol.* **2017,** *53*, 1116-1122.
30. Ye, Z. P.; Ling, Y.; Yu, Q.; Duan, H. L.; Kang, H. J.; Huang, G. M.; Duan, S. H.; Chen, X. M.; Liu, Y. G.; Zhou, S. X. Quantifying light response of leaf-scale water-use efficiency and its interrelationships with photosynthesis and stomatal conductance in C_3 and C_4 species. *Front. Plant Sci.* **2020,** *11*, 374.
31. Xu, Z.; Yin, H.; Xiong, P.; Wan, C.; Liu, Q. Short-term responses of *Picea asperata* seedlings of different ages grown in two contrasting forest ecosystems to experimental warming. *Environ. Exp. Bot.* **2012,** *77*, 1-11.
32. Yang, X. L.; Dong, W.; Liu, L. H.; Bi, Y. H.; Xu, W. Y.; Wang, X. Uncovering the differential growth of *Microcystis aeruginosa* cultivated under nitrate and ammonium from a pathophysiological perspective. *ACS ES&T Water* **2023,** *3*, 1161-1171.
33. Yang, X. L.; Liu, L. H.; Yin, Z. K.; Wang, X. Y.; Wang, S. B.; Ye, Z. P. Quantifying photosynthetic performance of phytoplankton based on photosynthesis–irradiance response models. *Environ. Sci. Eur.* **2020,** *32*, 24.
34. Smyth, T. J.; Pemberton, K. L.; Aiken, J.; Geider, R. J. A methodology to determine primary production and phytoplankton photosynthetic parameters from Fast Repetition Rate Fluorometry. *J. Plankton Res.* **2004,** *26*, 1337-1350.
35. Silsbe, G. M.; Kromkamp, J. C. Modeling the irradiance dependency of the quantum efficiency of photosynthesis. *Limnol. Oceanogr. - Meth.* **2012,** *10*, 645-652.
36. Buckley, T. N.; Diaz-Espejo, A. Reporting estimates of maximum potential electron transport rate. *New Phytol.* **2015,** *205*, 14-17.
37. Krall, J. P.; Edwards, G. E. Relationship between photosystem II activity and CO_2 fixation in leaves. *Physiologia Plantarum* **1992,** *86*, 180-187.

 doi:10.20944/preprints202504.1853.v1

38. Yu, H.; Niu, Y.; Hu, Y.; Du, D. Photosynthetic response of the floating-leaved macrophyte *Nymphoides peltata* to a temporary terrestrial habitat and its implications for ecological recovery of Lakeside zones. *Knowl. Manag. Aquat. Ec.* **2014,** *412*, 08.
39. Zhao, S.; Ruan, F.; Shen, W.; Deng, K.; Jiang, T.; Wu, P.; Feng, K.; Li, L. The effect of nitrogen fertilizer on rhizome quality and starch physicochemical properties in *Nelumbo nucifera*. In *Agronomy* **2022**, *12*, 794.
40. An, S.; Liu, X.; Wen, B.; Li, X.; Qi, P.; Zhang, K. Comparison of the photosynthetic capacity of Phragmites australis in five habitats in saline–alkaline wetlands. *Plants* **2020,** *9*, 1317.
41. Xu, J. Z.; Yu, Y. M.; Peng, S. Z.; Yang, S. H.; Liao, L. X. A modified nonrectangular hyperbola equation for photosynthetic light-response curves of leaves with different nitrogen status. *Photosynthetica* **2014,** *52*, 117-123.
42. Tiemuerbieke, B.; Ma, J.-Y.; Sun, W. Differential eco-physiological performance to declining groundwater depth in Central Asian C_3 and C_4 shrubs in the Gurbantunggut Desert. *Front. Plant Sci.* **2024,** *14*.
43. Luo, J.; Yang, Z.; Zhang, F.; Li, C. Effect of nitrogen application on enhancing high-temperature stress tolerance of tomato plants during the flowering and fruiting stage. *Front. Plant Sci.* **2023,** *14*, 1172078.
44. Zheng, M.; Mu, W.; Wang, Q.; Zhang, J.; Bai, Y.; Sun, Y.; Lu, Z.; Wei, X. Case study on the effects of sodium carboxymethyl cellulose and biostimulants on physiological and photosynthetic characteristics, yield, and quality of apples. *Agronomy* **2024,** *14*, 1403.
45. Ye, Z. P.; Stirbet, A.; An, T.; Robakowski, P.; Kang, H. J.; Yang, X. L.; Wang, F. B. Investigation on absorption cross-section of photosynthetic pigment molecules based on a mechanistic model of the photosynthetic electron flow-light response in C_3, C_4 species and cyanobacteria grown under various conditions. *Front. Plant Sci.* **2023,** *14*, 1234462.
46. Ye, Z.-P.; An, T.; Govindjee, G.; Robakowski, P.; Stirbet, A.; Yang, X.-L.; Hao, X.-Y.; Kang, H.-J.; Wang, F.-B. Addressing the long-standing limitations of double exponential and non-rectangular hyperbolic models in quantifying light-response of electron transport rates in different photosynthetic organisms under various conditions. *Front. Plant Sci.* **2024,** *15*, 581851.